Supplementary Material for manuscript

Reversible Water Driven Chirality Inversion in Cellulose-based Helices from *Erodium* Awns

Ana Almeida, Lara Querciagrossa, Pedro E. S. Silva, Filipa Gonçalves, João Canejo, Pedro L. Almeida, Maria Helena Godinho* and Claudio Zannoni*

Correspondence to: mhg@fct.unl.pt and Claudio.Zannoni@unibo.it

This PDF file includes:

Supplementary Text
Supplementary Figures S1 to S4
Captions for Movies S1 to S6

Other Supplementary Materials for this manuscript include the following:

Movies S1 to S6

Supplementary Text and Figures

Winding and unwinding behaviors and structural characteristics of pristine *Erodium* seeds were investigated. Similar results as those found in literature for different *Erodium* seeds were also obtained for the *Erodium* seeds collected in Portugal (Caparica region), shown in Fig. S1. No left-handed helices were obtained upon hydration of the awns.

Analysis of molecular dynamics simulations have been carried on using the overall evolution approach described in the main text to follow the changes in the shape of a whole elastic filament in time. During the compression stage, when the rod curls and adopts a right-handed helical shape, the chirality index assumes positive values. When the modified bonds start to expand and the structure starts to reverse the coiling, the G^a decreases, reaching a minimum of the opposite sign and about the same magnitude, Fig. S2.

The dynamics of ribbons upon contraction and swelling is explained by using a simple model. A typical array of beads used in simulations is shown in Fig. S3. First and second neighbor beads are elastically connected. The asymmetric contraction is generated by modifying bonds colored in red, as shown in Fig. S3.

The active structure, extracted from the pristine awn, change chirality from right-handed (un-hydrated state) to left-handed (hydrated state) helices and is transparent and highly birefringent when wet (Fig. S4, POM results).

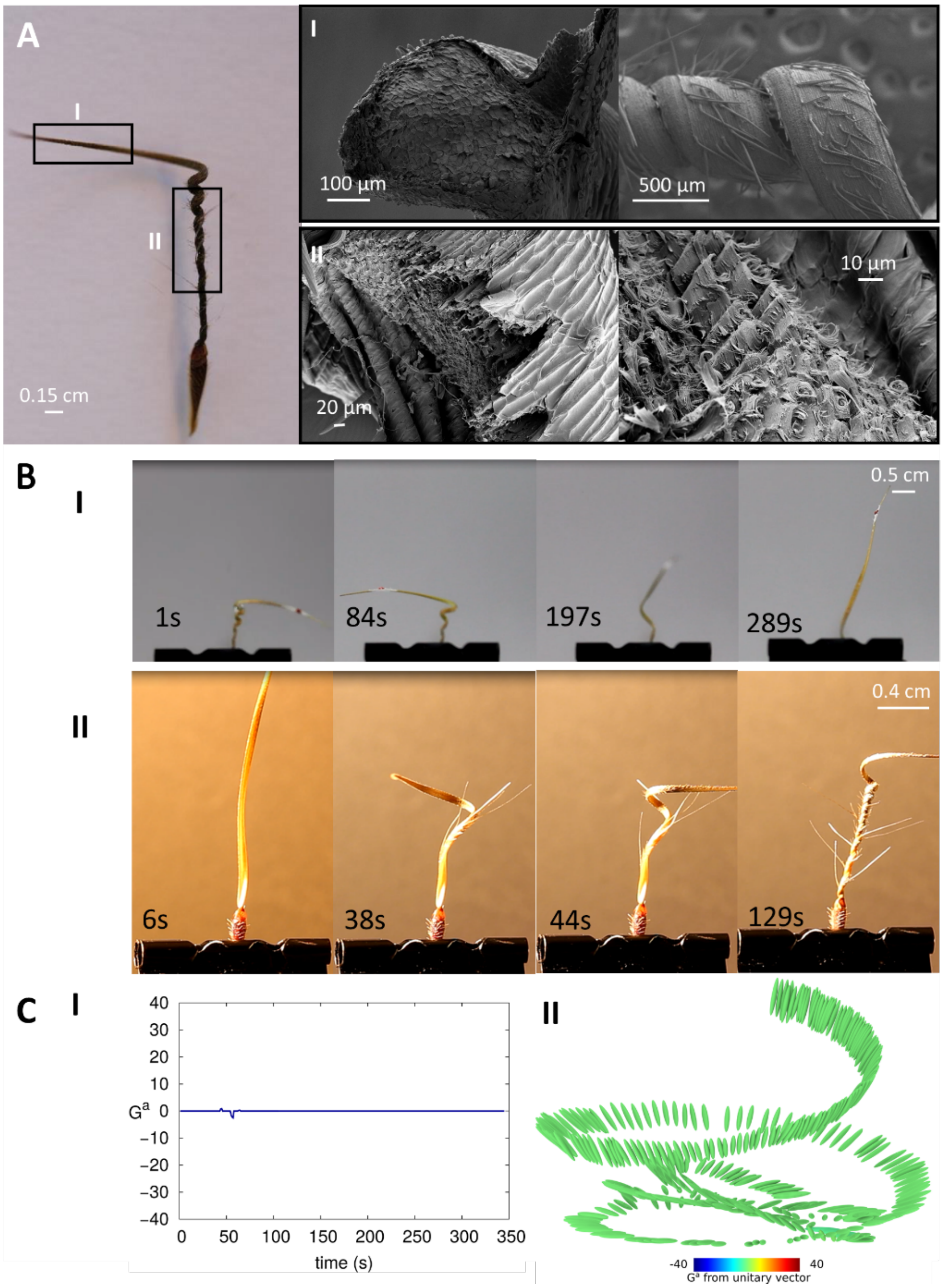

Fig. S1: **Structure and reversible hygroscopic *Erodium* awns movements**: anticlockwise helical (dry) and straight (wet) shapes. (A) dry awn with seed, the tail (I and SEM picture of the cross section, on top left) and the coiling region (II and SEM pictures with outer surface and cross sections details, on the left) are shown. (B) I: the awn is dipped in a container with water; it uncoils from an anticlockwise helix to a straight shape. II: the awn is dried in a controlled atmosphere and temperature environment (T = 60 °C), returning to a R helix. (C) chirality index versus time (I) and a snapshot of the movie (II) built from position, described by the application point, and orientation, as in the unitary vector, color–coded using chirality index values. As expected, there are no great fluctuations, since chirality remains stable during hydration and drying of the awn.

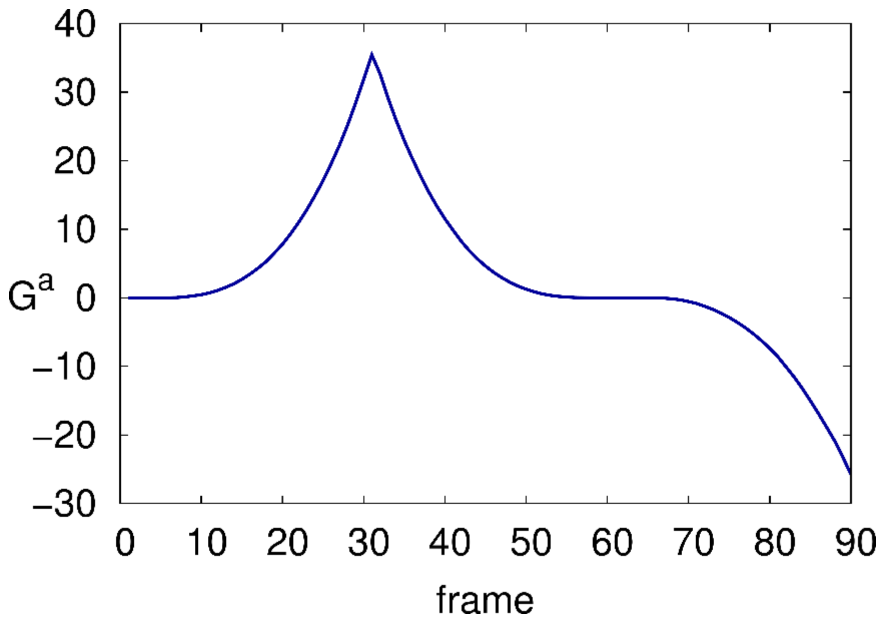

Fig. S2: **Overall chirality evolution with time.** Analysis of the shape of the elastic model filament investigated with LAMMPS shows that during the compression stage, when the rod curls and adopts a right-handed helical shape, the chirality index G^a assumes positive values. As the modified bonds start to expand and the structure reverses the coiling, G^a decreases, reaching a minimum with the opposite sign.

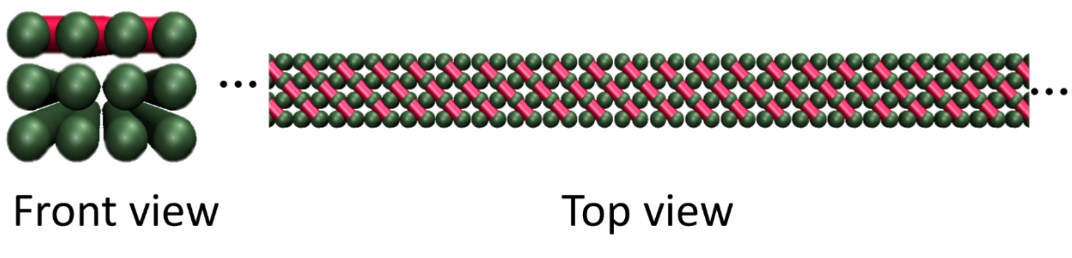

Fig. S3: **Array of beads used in simulations.** Elastic filaments were modeled as beads arranged in a simple cubic lattice and bonded to firsts and seconds neighbors. Asymmetry along the filament was generated by modifying the equilibrium bond distances of specific second neighbors, as illustrated with red cylinders.

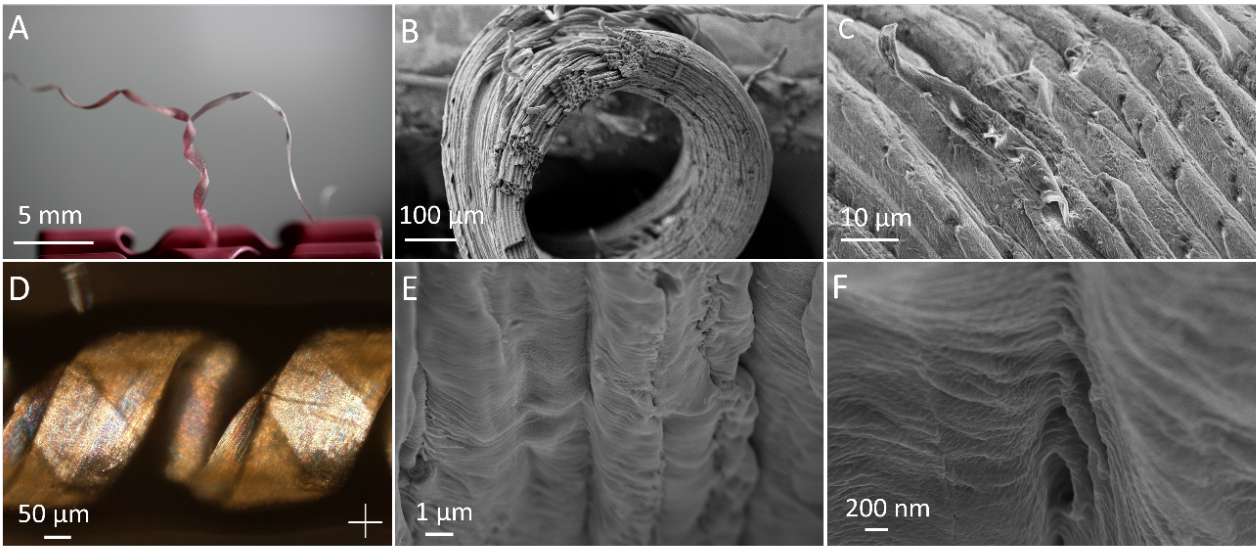

Fig. S4: **Active layer in chemically treated ribbons.** (A) Dry ribbon after chemical treatment and swelling in a red dye. Inner (pink ribbon) and outer (whitish ribbon) layers can be isolated. (B) and (C) SEM pictures of tubes (R helix) and of the tubes surface, of the dry inner layer. (D) POM picture of the wet (L helix) ribbon, between cross polarizers showing the two birefringent transparent layers The wrinkles at the tubes surface and details of the nano structure showing cellulose nano fibrils are given in (E) and (F).

Movie Captions

Movie S1: MRI animation .gif of slices of the *Erodium* wet fruit along its main axis.

Movie S2: 3D MRI movie of the *Erodium* fruit

Movie S3: Time-lapse movies of an *Erodium* seed explosive dispersal from fruit

Movie S4: Hydration of an awn in an alkali water solution (5% w/w) (speed:8x). The movements of the awn are highlighted by a red dot.

Movie S5: Hydration of an inner treated ribbon in water.

Movie S6: Molecular dynamics simulation showing the switch between right- and left-handedness of a ribbon being stretched and unstretched diagonally relatively to its main axis.